2021 IEEE 4th International Conference on Computing, Power and Communication Technologies (GUCON)
University of Malaya, Kuala Lumpur, Malaysia. Sep 24-26, 2021

2021 IEEE 4th International Conference on Computing, Power and Communication Technologies (GUCON) | 978-1-7281-9951-1/21/$31.00 ©2021 IEEE | DOI: 10.1109/GUCON50781.2021.9573805

Sliding Mode Control of Two-Switch Buck Boost Non-Isolated On-Board Battery Charger

Bonela Anil Kumar
Department of Electrical Engineering
National Institute of Technology Manipur
Imphal, India
anilk193@gmail.com

Mrinal Kanti Sarkar
Department of Electrical Engineering
National Institute of Technology Manipur
Imphal, India
mks_ee@ieee.org

***Abstract* - This paper presents the application of sliding mode control for a two-switch buck-boost (TSBB) non isolated on-board battery charger operating over a wide range of output voltages. A two-loop control scheme with PI in the outer loop and reduced order SMC in the inner loop is used to achieve the control objectives of tight output voltage regulation, high power factor and robustness of the control scheme. The complexity in the design and implementation of SMC was reduced by using Hankel model reduction method. Simulation was carried out on PSIM and MATLAB software to obtain comparative analysis of PI-SMC and PI-PI control Scheme. The PI-SMC showed good dynamic response and robust performance over PI-PI control scheme.**

***Index Terms*— sliding mode control, TSBB, OBC, Hankel model**

I. INTRODUCTION

There is a growing interest in developing efficient, small in volume and cost-effective charging solutions for electric vehicles. These are the key characteristics for their wider acceptance and penetration in the market. The on-board battery charger typically is a two-stage converter, with front end ac-dc PFC stage followed by back-end DC-DC stage. A high frequency galvanic isolation is provided in DC-DC stage to isolate the battery from ac grid. The high frequency isolation however had a negative influence on the efficiency and power density of the converter [1]. Non-isolated battery chargers are gaining much interest due to low weight, size and cost. Non-isolated topologies with single switch configurations such as buck–boost converters, SEPIC, Cuk, Zeta converters have problems in implementation over wide range of output voltages and power levels. Apart from this there is also a problem of reversal of ground between input and output in the absence of galvanic isolation [2]. Many two-switch topologies such as the buck cascaded buck-boost (BuCBB), boost cascaded buck-boost (BoCBB), and boost interleaved buck-boost (BoIBB) converters have been proposed in literature for wide range of output voltage and power levels [3]. The problem of reversal of ground between input and output can be addressed by isolating the insulation fault with relays and breakers during charging. Control methods like current-programmed control (CPC) [4], peak current-mode control (PCMC), Average current mode control (ACMC) [5] were used with different type of cascaded controllers. These cascade control schemes were was mostly investigated with single-switch topologies with limited voltage control. Sliding mode control of late has gained a lot of attention in the control of power converters because of its ability to handle uncertainties, non-linearities and inherent robust performance capabilities with good dynamic performance [6]. In this study, a non-isolated two-switch buck-boost (TSBB) configuration is considered for OBC. The problem of good voltage regulation with high input power factor for wide range of output voltages is addressed by choosing a two-loop control structure with PI controller in the outer voltage loop and sliding mode controller in the inner current loop. The performance of the controller is assessed in terms of voltage regulation, input power factor and robustness in the presence of bounded disturbance.

II. MODELLING OF TSBB CONVERTER

The circuit diagram of non-isolated TSBB converter with boost and buck cell in cascaded configuration is shown in Fig. 1. The controlled switches of boost and buck cell are controlled independently depending upon the operating output voltage. Basically, there are two modes of operation based on the input voltage and the dc output voltage.

Mode A ($V_0 > V_d$)

In this mode with the input voltage less than the DC output voltage, the components of boost cell come into conduction state. A PWM signal is applied to switch S_1 keeping switch S_2 always in on condition. The state dynamics of the converter described by state space averaging method is given by

$$\dot{X} = AX + BU \tag{1}$$

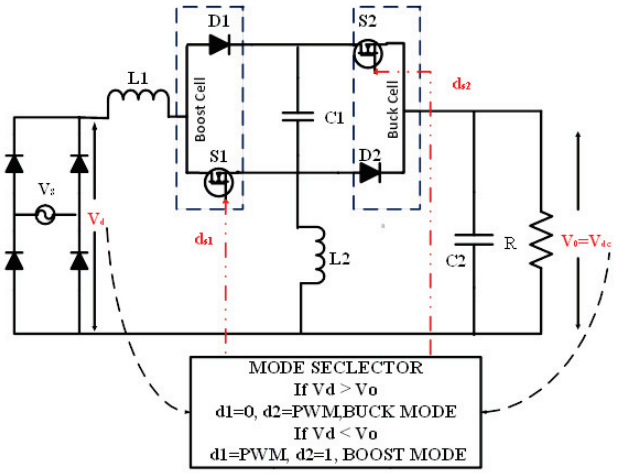

Fig. 1. Non isolated TSBB Converter

$$\begin{pmatrix} \frac{di_{L1}}{dt} \\ \frac{di_{L2}}{dt} \\ \frac{dV_{c1}}{dt} \\ \frac{dV_{c2}}{dt} \end{pmatrix} = \begin{pmatrix} 0 & 0 & \frac{d_1}{L_1} & -\frac{1}{L_1} \\ 0 & 0 & -\frac{1}{L_2} & \frac{1}{L_2} \\ -\frac{d_1}{C_1} & \frac{1}{C_1} & 0 & 0 \\ \frac{1}{C_2} & -\frac{1}{C_2} & 0 & -\frac{1}{RC_2} \end{pmatrix} \begin{pmatrix} i_{L1} \\ i_{L2} \\ v_{C1} \\ v_{C2} \end{pmatrix} + \begin{pmatrix} \frac{1}{L_1} \\ 0 \\ 0 \\ 0 \end{pmatrix} V_d \quad (2)$$

Mode B ($V_0<V_d$)

The buck cell comes into conduction state whenever the input voltage is greater than the DC output voltage. The PWM pulses are applied to S_2 keeping the switch S_1 always in off state. The state dynamics of the converter in this mode is described by the following state model

$$\begin{pmatrix} \frac{di_{L1}}{dt} \\ \frac{di_{L2}}{dt} \\ \frac{dV_{c1}}{dt} \\ \frac{dV_{c2}}{dt} \end{pmatrix} = \begin{pmatrix} 0 & 0 & -\frac{(1-d_2)}{L_1} & -\frac{1}{L_1} \\ 0 & 0 & \frac{d_2}{L_2} & -\frac{1}{L_2} \\ \frac{(1-d_2)}{C_1} & -\frac{d_2}{C_1} & 0 & 0 \\ \frac{1}{C_2} & \frac{1}{C_2} & 0 & -\frac{1}{RC_2} \end{pmatrix} \begin{pmatrix} i_{L1} \\ i_{L2} \\ v_{C1} \\ v_{C2} \end{pmatrix} + \begin{pmatrix} \frac{1}{L_1} \\ 0 \\ 0 \\ 0 \end{pmatrix} V_d \quad (3)$$

A. Design of Parameters

The inductors L_1 and L_2 of TSBB converter have to be designed in such a way the load current should be continuous with low ripple content. Capacitor C_1 is a key component in both buck and boost mode of operation, responsible for low voltage ripple across C_1 during boost operation and acts as input filter in combination with L_1 during buck mode. The selection of capacitor C_2 is based on the requirement of stiff voltage at the output with a low-frequency output voltage ripple. [7]

$$L_1 > \frac{R_e}{2f_s}\left(1-\frac{|V_s|}{V_d}\right) \quad (4)$$

$$C_1 = \frac{|V_s|}{R_e \nabla V_{c1} f_s}\left(1-\frac{|V_s|}{V_d}\right) \quad (5)$$

$$C_2 \geq \frac{P}{2\pi f_s V_d \nabla V_d} \quad (6)$$

$$L_{eq} = (L_1 \,||\, L_2) > \left(\frac{R_e(|V_s|-V_d)V_d^{\,2}}{2(|V_s|)^3}\right) \quad (7)$$

III. CONTROL STRUCTURE

The cascade control scheme shown in Fig. 2 allows independent control of switches in both modes (Mode A and Mode B) of operation. The voltage control loop generates the current reference i_{ref} by multiplying voltage error with |sin ωt| along with reciprocal of feedforward input voltage constant. The sliding mode current controller in the inner loop generates PWM signal based on the error between the reference current and the inductor current i_{L1}.The reference current tracking is done at switching frequency and the average output voltage is regulated over the line frequency. Thus, in two-loop control structure the bandwidth of inner current loop is ten times or more higher than outer voltage loop [8]. The mode selector block allows independent control of boost and buck modes based on input and output voltage conditions.

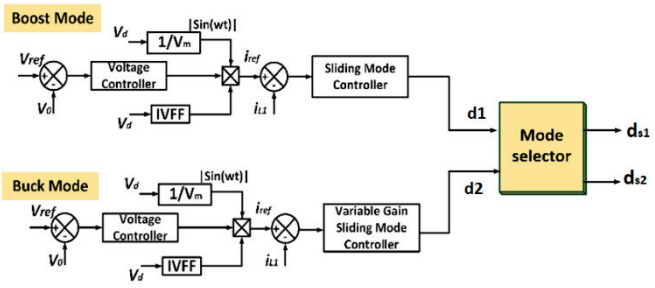

Fig. 2. Control scheme for two mode TSBB converter

A. Model Reduction Using Hankel Singular Values (HSV)

Model reduction using HSV reduces the full-size model to a smaller size, such that it is practically feasible for implementation while maintaining the modeling accuracy. The closed loop control of TSBB converter needs the measurement of four state variables, measurement of all four state increases the cost and complexity of controller design while implementation. Therefore, the complexity of controller design can be reduced by converting the fourth order system to second order system using Hankel model reduction technique [9],[10],[11].

B. Design of Sliding Mode Controller

The design objective is to choose variable S and related discontinuous control law such that the error state vector attains sliding mode in finite time. The sliding function is chosen to be linear combination of error state variables.

$$S(e) = \lambda_1 e_1 + \lambda_2 e_2 = [\lambda][e] \quad (8)$$

Let Z represent the reference vector $Z = [z_1 \;\; z_2]^T$ where $z_1 = V_{ref}$, $z_2 = i_{ref}$ and X the measured state variables $X = (x_1 \;\; x_2)^T$ where $x_1 = v_o$, $x_2 = i_{L1}$ and e the error vector. $S(e) = [\lambda][e]$,where sliding coefficients $\lambda_1, \lambda_2 > 0$ and

$$e = Z - X \quad (9)$$

Differentiating (9) with respect to time and substituting (1), we obtain

$$\dot{e} = \dot{Z} - AX - Bu \quad (10)$$

From (9) we can write $X = Z - e$ and substituting X in (10), $\dot{e}$ can be expressed as

$$\dot{e} = \dot{Z} - AZ + Ae - Bu \tag{11}$$

We have the ideal sliding mode defined by $S = \dot{S} = 0$ and the continuous control u_{eq} which maintains ideal sliding motion during sliding phase is derived from

$$\begin{aligned} &\dot{S}\big|_{u=u_{eq}} = 0 \\ &\dot{S}(e) = [\lambda][\dot{e}] = [\lambda][\dot{Z} - AZ + Ae - Bu_{eq}] = 0 \end{aligned} \tag{12}$$

Thus, the equivalent control derived in terms of sliding coefficients and error state vector is given as

$$u_{eq} = [\lambda B]^{-1}\lambda[\dot{Z} - AZ + Ae] \tag{13}$$

Substituting (13) in (11) and by applying the invariance condition $\dot{Z} - AZ = 0$,the error dynamics can be given as

$$\begin{aligned} &\dot{e} = [I - B(\lambda B)^{-1}\lambda][\dot{Z} - AZ + Ae] \\ &\dot{e}(t) = [I - B(\lambda B)^{-1}\lambda]Ae(t) \end{aligned} \tag{14}$$

$$\dot{e}(t) = A_{eq}e(t) \tag{15}$$

The error dynamics in equation (15) of output voltage and inductor current can achieve asymptotic convergence at desired rate based on the eigenvalues of A_{eq}. The sliding coefficients are calculated from the eigen values of the $A_{eq,}$ for mode A and mode B of operation. The switching function employed to bring the state trajectory of the system at any initial position to the sliding surface is given as

$$u(t) = \rho sign(s) \tag{16}$$

It is found that chattering effect of the sliding mode controller is prominent in buck-boost mode of operation *(Mode B*). Chattering reduces the control accuracy and the controlled variables oscillate around the reference value. This problem can be avoided by replacing fixed gain SMC with variable gain SMC. The switching gain is now a function of magnitude of sliding variable

$$u = u_{eq} + \rho(s)sign(s) \tag{17}$$

$$\text{where } \rho(s) = \frac{1}{(1 + \frac{1}{|s|})e^{-|s|}} \tag{18}$$

As s becomes zero, value of switching gain becomes zero at the sliding surface and the chattering will be eliminated at steady state.

IV. SIMULATION RESULTS

The TSBB converter is simulated using PSIM and MATLAB software. The voltage controller in the outer loop and reduced order SMC in inner loop is designed with the parameters in Table 1.

TABLE I. PARAMETERS OF THE CONVERTER

Parameter	Value
Input voltage $V_{s(rms)}$	120V,50Hz
Output voltage V_o	150-400V
Switching frequency	30kHz
Inductor L_1	3mH
Inductor L_2	0.252 mH
Capacitor C_1	80uf
Capacitor C_2	95uf
Load R	22.5 -100Ω

The PI controller in the outer loop is designed such that it responds to a wide range of output voltages. The transfer function of PI controller for mode A and mode B operation is obtained as follows.

$$G_{VA}(s) = \frac{7.43(1 + 0.098s)}{0.098s} \tag{19}$$

$$G_{VB}(s) = \frac{1.43(1 + 0.098s)}{0.098s} \tag{20}$$

The SMC in the inner loop is designed with second order state model obtained through Hankel model reduction technique using the state energy diagram shown in Fig. 3. The state model obtained for mode A and mode B of operation is given below

$$\text{For boost mode } A = \begin{pmatrix} 0 & 1 \\ -9503 & -5.1 \end{pmatrix} \quad B = \begin{pmatrix} 0 \\ 1 \end{pmatrix} \tag{21}$$

$$\text{For buck mode } A = \begin{pmatrix} 0 & 1 \\ -38354 & -1 \end{pmatrix} \quad B = \begin{pmatrix} 0 \\ 1 \end{pmatrix} \tag{22}$$

Using (15), (21), (22), the sliding coefficients for mode A and mode B of operation are obtained as given in (23) such that asymptotic convergence of error to zero is achieved at the desired rate.

$$\lambda_{\text{mode}A} = (1 \quad 0.5) \text{ and } \lambda_{\text{mode}B} = (1 \quad 0.09) \tag{23}$$

The TSBB converter is fed with 170V peak input supply with a load resistance R=45Ω. For a reference voltage V_{ref} equal to 400V and 200V respectively, the converter operates in mode A

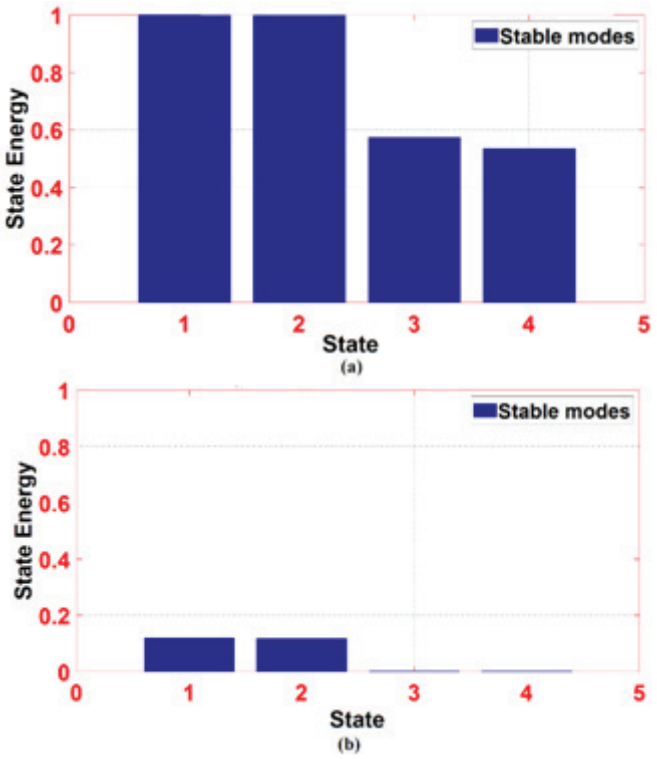

Fig. 3. Hankel Singular value (state contribution), (a) Mode A, (b) Mode B

and in mode B for V_{ref} equal to 150V. Fig.4(a) to (c) shows the comparative simulation results of proposed control scheme (PI-SMC) with a control structure containing PI controller in both inner and outer loop (PI-PI). The controller gains of PI-PI control scheme are taken from [7]. In Mode A (V_o>V_d) with a reference voltage of 400V and 200V respectively, the proposed control scheme has low rise time, less overshoot (< 8%) and less settling time (< 2 secs). However, with PI-PI control scheme the system response was slow with large settling time. In Mode B (V_o<V_d) with a reference voltage of 150V, PI-PI control scheme has more ripple and overshoot in output voltage than in PI-SMC control scheme. The PI-SMC control scheme has an input power factor of 0.991 and 0.84 respectively for Mode A and Mode B of operation as shown in Fig.5 (a) and 5(b). The PI-PI control scheme also had near about same values in both modes of operation. A step change in load is incorporated by reducing the load resistance to half of its earlier value. For a reference voltage of 200V, with PI-SMC control the transient settles down at a faster rate than that of PI-PI control scheme without any change in its steady state value as shown in Fig.6(a), (b). However, for a reference voltage of 150V, with PI-PI control the output voltage reduces by 3% for an increase of load by 50% but with PI-SMC control, the output voltage maintains its steady state value after the transient as shown in Fig.6(c). With a bounded disturbance of $d(t) = 15\sin \omega t$ introduced into the plant, the PI-SMC scheme shown no significant change in the output voltage as shown in Fig.7(a). However, with PI-PI control scheme an overshoot of around 50 % and large pulsation as shown in Fig.7(b) is seen in steady state output voltage. Therefore PI-SMC control was more effective in rejecting the disturbances in comparison with PI-PI control scheme.

V. CONCLUSION

In this paper TSBB non-isolated converter for a wide range of voltages has been analyzed with a control structure that provides independent control of boost and buck mode of operation. For simplicity of implementation, fourth order state space model is reduced to a second order model using Hankel model reduction method in the design of inner loop SMC. The chattering effect in buck-boost mode (Mode B) of operation is reduced by replacing fixed gain SMC (Mode A) with variable gain SMC. Simulation was carried out for a wide range of output voltages 150-400V with input peak voltage of 170V under normal and under a sudden load change condition. A comparative analysis of simulation results with PI-SMC and PI-PI control scheme was performed. The proposed PI-SMC control scheme shown good dynamic response and voltage regulation over wide range of output voltages. A nearly unity PF for boost mode but slightly lower PF for buck mode is observed with both PI-SMC and PI-PI control scheme. Further the proposed control scheme PI-SMC shown robust performance against bounded disturbance over PI-PI scheme. However, during implementation uncertainties such as imprecision in controller coefficients can affect the controller performance and these are unavoidable due the finite word length of digital controllers. To address such problems in implementation, the effectiveness of non-fragile controllers can be investigated.

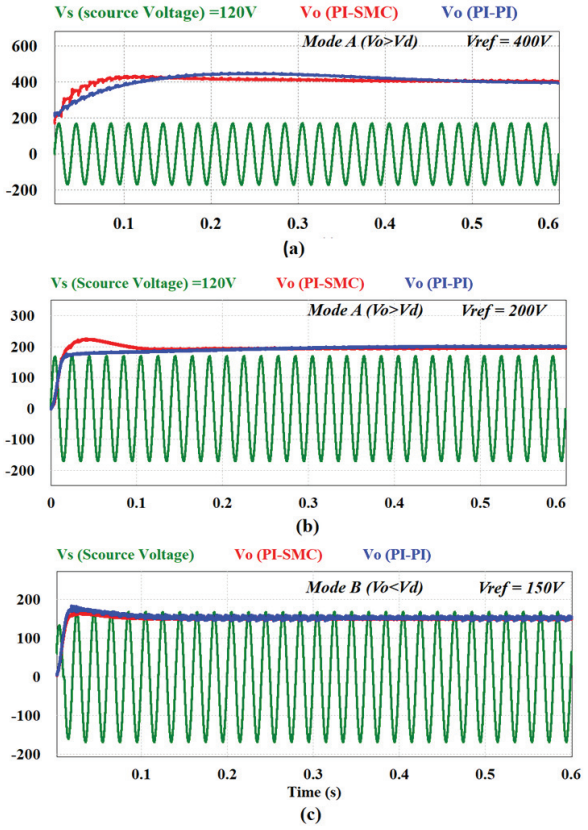

Fig. 4. Input and Output voltages of Mode A and Mode B of converter operation

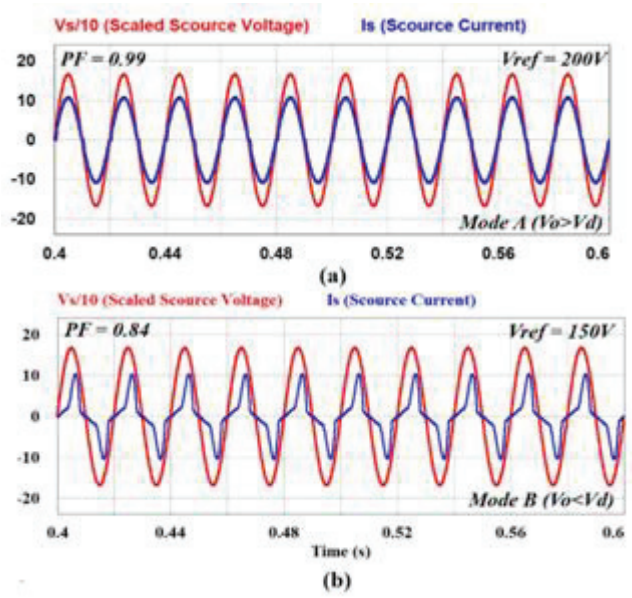

Fig. 5. Plot of scaled input voltage and source current, (a) Mode(A), (b) Mode (B).

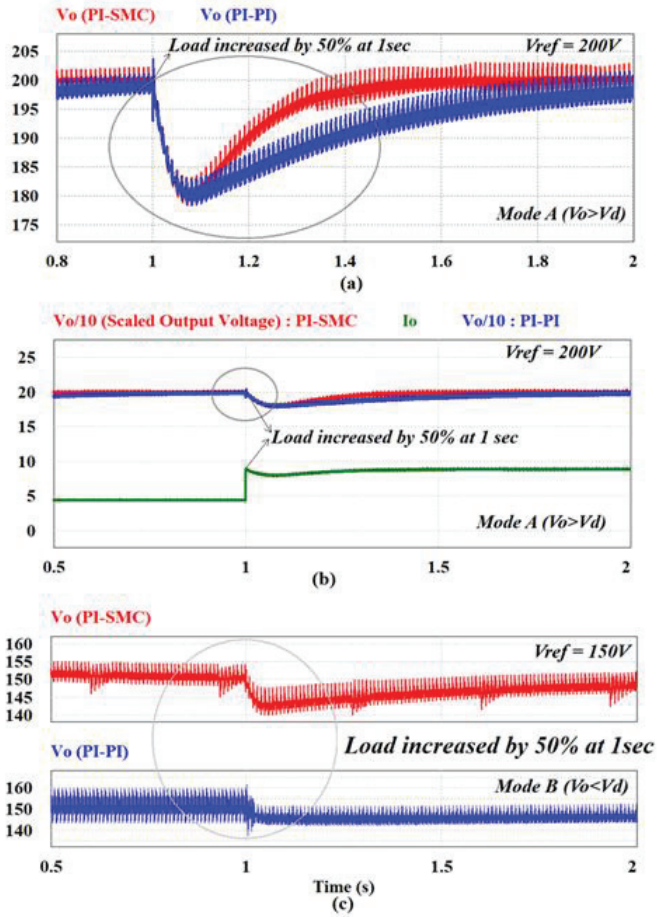

Fig. 6. (a), (b), (c) Output voltages of Mode A and Mode B under sudden change in load

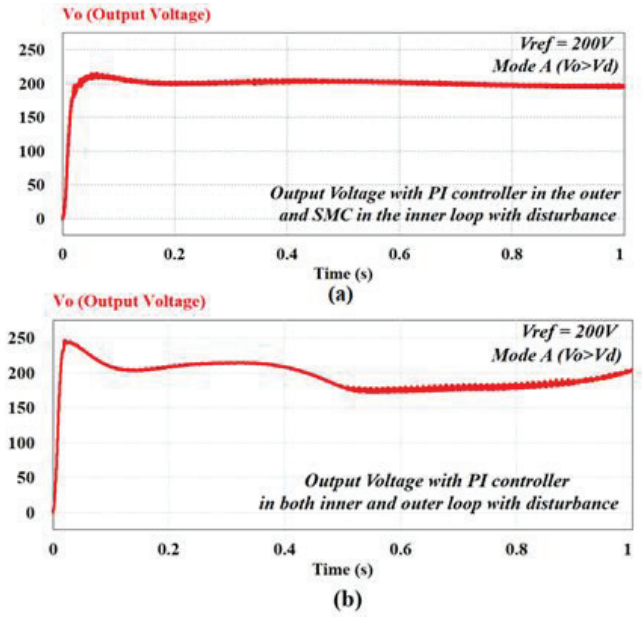

Fig. 7. Output voltages of the converter with bounded disturbance, (a) PI-SMC, (b) PI-PI.

REFERANCES

[1] Rivera S, Kouro S, Wu B, "Charging Architectures for Electric and Plug-In Hybrid Electric Vehicles," Technologies and Applications for Smart Charging of Electric and Plug-in Hybrid Vehicles. Springer, Cham. 2017

[2] C. Oh, D. Kim, D. Woo, W. Sung, Y. Kim and B. Lee, "A High-Efficient Non isolated Single-Stage On-Board Battery Charger for Electric Vehicles," IEEE Transactions on Power Electronics, vol. 28, no. 12, pp. 5746-5757, Dec. 2013

[3] T. Bang and J. Park, "Development of a ZVT-PWM Buck Cascaded Buck–Boost PFC Converter of 2 kW With the Widest Range of Input Voltage," IEEE Transactions on Industrial Electronics, vol. 65, no. 3, pp. 2090-2099, March 2018.

[4] G. K. Andersen and F. Blaabjerg, "Current programmed control of a single-phase two-switch buck-boost power factor correction circuit," IEEE

[5] D. S. Gautam, F. Musavi, M. Edington, W. Eberle, and W. G. Dunford, "An automotive onboard 3.3-kW battery charger for PHEV application," IEEE Trans. Veh. Technol., vol. 61, no. 8, pp. 3466–3474, Oct 2012.

[6] Abdelhalim Kessal, Lazhar Rahmani, "Analysis and design of sliding mode controller gains for boost power factor corrector," Volume 52, Issue 5, Pages 638-643, 2013

[7] A. V. J. S. Praneeth and S. S. Williamson, "Modeling, Design, Analysis, and Control of a Non isolated Universal On-Board Battery Charger for Electric Transportation," IEEE Transactions on Transportation Electrification, vol. 5, no. 4, pp. 912-924, December 2019.

[8] Chu, G., Tan, S.-C., Tse, C.K. and Wong, S.C, " Robust current control for boost PFC converters from a sliding mode viewpoint," Int. J. Circ. Theory. Appl., 39: 543-556, 2011.

[9] Safonov, M.G., and R.Y. Chiang, "A Schur Method for Balanced Model Reduction," IEEE Trans. on Automat. Contr., vol. AC-2, no. 7, pp. 729-733, July 1989.

[10] M. G. Safonov, R. Y. Chiang and D. J. N. Limebeer, "Optimal Hankel model reduction for nonminimal systems," in IEEE Transactions on Automatic Control, vol. 35, no. 4, pp. 496-502, April 1990.

[11] C. B. Vishwakarma "Modified Hankel Matrix Approach for Model Order Reduction in Time Domain," World Academy of Science Engineering and Technology International Journal of Physical and Mathematical Sciences Vol:8, No:2, 2014.

[12] M G Maheshwari, G Uma, KM Vijayalakshmi, " Design and implementation of reduced-order sliding mode controller for higher-order power factor correction converters" IET power electronics Volume 4, Issue 9, p. 984 – 992, November 2011.

[13] A. Mallik, J. Lu and A. Khaligh, "Sliding Mode Control of Single-Phase Interleaved Totem-Pole PFC for Electric Vehicle Onboard Chargers," in IEEE Transactions on Vehicular Technology, vol. 67, no. 9, pp. 8100-8109, Sept. 2018

[14] C. Yao, X. Ruan, W. Cao and P. Chen, "A Two-Mode Control Scheme with Input Voltage Feed-Forward for the Two-Switch Buck-Boost DC–DC Converter," in IEEE Transactions on Power Electronics, vol. 29, no. 4, pp. 2037-2048, April 2014

[15] Bouafassa, A., L. Rahmani and S. Mekhilef. "Design and real time implementation of single-phase boost power factor correction converter." ISA transactions 55 (2015): 267-74 .

[16] R. Pandey and B. Singh, "A Power Factor Corrected Electric Vehicle Battery Charger Using Boost Converter," 2018 8th IEEE India International Conference on Power Electronics (IICPE), pp. 1-6, 2018

[17] Das, Souvik, Mohd Salim Qureshi and Pankaj Swarnkar. "Design of integral sliding mode control for DC-DC converters." Materials Today: Proceedings 5 (2018): 4290-4298.

[18] Siew-Chong Tan, Y. M. Lai and C. K. Tse, "A unified approach to the design of PWM-based sliding-mode voltage controllers for basic DC-DC converters in continuous conduction mode," in IEEE Transactions on Circuits and Systems I: Regular Papers, vol. 53, no. 8, pp. 1816-1827, Aug. 2006

[19] Taheri, B., Sedaghat, M., Bagherpour, M.A. et al. A New Controller for DC-DC Converters Based on Sliding Mode Control Techniques. J Control Autom Electr Syst 30, 63–74, 2019

[20] C. -Y. Oh, D. -H. Kim, D. -G. Woo, W. -Y. Sung, Y. -S. Kim, and B.-K. Lee, "A high-efficient non-isolated single-stage on-board battery charger for electric vehicles," IEEE Trans. Power Electron., vol. 28, no. 12, pp. 5746– 5757, Dec. 2013

[21] Arulselvi S, Uma G, ChidambaramM. Design of PID controller for boost converter with RHS zero. In: Proceeedings of the 4th International PowerElectronics and Motion Control Conference (IPEMC 2004), China; 2004